Aleksandar Živković[1], Andrijana Đurđević[2], Aleksandar Sedmak[3], Srđan Tadić[2], Ivan Jovanović[1], Đorđe Đurđević[4], Kenneth Zammit[5]

FRICTION STIR WELDING OF ALUMINIUM ALLOYS – T JOINTS

ZAVARIVANJE TRENJEM SA MEŠANJEM ALUMINIJUMSKIH LEGURA – T SPOJEVI

Originalni naučni rad / Original scientific paper
UDK /UDC: 621.791.1:669.715
Rad primljen / Paper received: 11.12.2015

Adresa autora / Author's address:
[1)] Goša FOM Company, Smederevska Palanka, Serbia
[2)] University of Belgrade, Innovation Centre of Faculty of Mechanical Engineering, Belgrade, Serbia, email: andrijana.miler@yahoo.com
[3)] University of Belgrade, Faculty of Mechanical Engng.
[4)] Tehnikum Taurunum - College of Applied Engineering Studies, Belgrade, Serbia
[5)] Malta College of Art, Science and Technology, Paola, Malta

Keywords
- friction stir welding (FSW)
- T-joints
- defects
- microhardness

Abstract

The paper presents results of research on the possibility of producing T-joints of aluminium alloys without defect by friction stir welding process. Friction stir welding process is applied in welding T-joints of aluminium alloys 5052-H32 and 5754-H111. These relatively new welding technologies produce high quality welded joints, where strength of the joint can reach the strength of the base material. Visual and macrostructural examination and microhardness measuring of the welded T-joints are processed.

Ključne reči
- zavarivanje trenjem sa mešanjem (ZTM)
- T spojevi
- greške
- mikrotvrdoća

Izvod

Predstavljeni su rezultati istraživanja mogućnosti proizvodnje T spojeva od aluminijumskih legura zavarivanjem trenjem sa mešanjem bez grešaka. Postupak zavarivanja trenjem sa mešanjem je korišćen za zavarivanje T spojeva od aluminijumskih legura 5052-H32 i 5754-H111. Ova relativno nova tehnologija zavarivanja daje visoko kvalitetne zavarene spojeve kod kojih čvrstoća spoja može dostići čvrstoću osnovnog materijala. Urađeno je vizuelno i makrostrukturno ispitivanje i merenje mikrotvrdoće T spojeva.

INTRODUCTION

Friction Stir Welding (FSW) is a solid-state welding process which enables joining of materials without melting and without the use of additional materials. Joining of material is performed by combined action of heat and mechanical work. Tool and base material stay in solid-state, while in the welding zone the base material is slightly softened. Temperatures during the process do not exceed the melting point of the base material, and those are about 80% of the melting point. Welding temperature for aluminium alloys are in the interval 400–500°C, /1-2/.

Relative to the traditional welding technologies, FSW offers a number of advantages, /3/. The introduction of FSW joining technology, simplifies the production scenario of particularly shaped profiles. In the aircraft and aerospace industries complex profiles and joining of so-called 'skin and stringers' are very often used for flying body structures. In recent years a few results have been presented that investigate the development of welded T-joints made of lightweight alloys, by using FSW, /4-5/. Here, experimental welding of aluminium plates is performed in order to obtain T-joints without defects.

EXPERIMENTAL RESEARCH

Experimental welding is performed on the milling machine, type AG-400 MINA. Rated power of the machine is 12 kW, the maximum rotational speed is 2500 min^{-1}, the maximum feed rate is 4500 mm/min and working space is x = 600 mm, y = 400 mm and z = 300 mm.

The tool for friction stir welding is of H13 tool steel. The welding tool has a typical geometry for the FSW process, cylindrical shoulder and tapered probe with a cone angle of 20°. The probe is an etched curvaceous right coil whose tilt is 5°, which promotes better mixing and secondary flow of softened material. Height of the probe is 5.5 mm. Diameter of shoulder is 25 mm. Top of shoulder is concave.

Experimental research had two phases because there were two different aluminium alloys. During the first experimental welding phase T-joints were produced by friction stir welding of three plates of aluminium alloy 5052-H32 of dimensions 30×180×5 mm. Chemical composition and mechanical properties of T-joints produced in the first phase of experimental welding are given in Tables 1 and 2, respectively. The following limits are given according to EN 485-2 and EN 573-3 standards.

Table 1. Chemical composition of AA5052-H32, /6/.

%	Cu	Mn	Mg	Si	Fe	Zn	Ti	Cr
min.	0	0	2.2	0	0	0	0	0.15
max.	0.1	0.1	2.8	0.25	0.4	0.1	0.01	0.35

Table 2. Mechanical properties of AA5052-H32, /7/.

Property	$R_{p0.2}$ (MPa)	R_m (MPa)	A (%)	HV5
Value	130	210-260	12	67

In the second welding phase T-joints are produced by welding three plates of AA 5754-H111, of dimensions 30× 180×5 mm and chemical composition, as given in Table 3, and mechanical properties given in Table 4. The following limits are given according to standards EN 485-2 and EN 573-3.

Table 3. Chemical composition of AA 5754-H111, /6/.

%	Mg	Mn	Si	Cu	Fe	Zn	Ti	Cr
min.	2.6	0	0	0	0	0	0	0
max.	3.6	0.5	0.4	0.1	0.4	0.2	0.015	0.3

Table 4. Mechanical properties of AA 5754-H111, /7/.

Property	$R_{p0.2}$ (MPa)	R_m (MPa)	A (%)	HB
Value	80	190-240	18	52

The design of the clamping tool for working plates is the same for both welding phases and is given in Fig. 1. Radiuses of backing plates are 2 mm. However, for welding of the T-joints of AA5052-H32, the material of clamping tool was carbon steel S355, according to EN 10025/2004 standard. Material of the clamping tool for welding T-joints of AA5754-H111 was stainless steel 1.430.

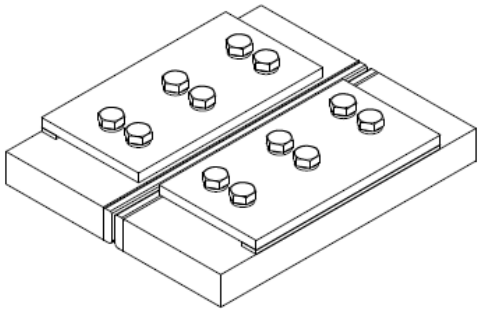

Figure 1. Simplified representation of the clamping tool.

There are five welding parameters that affect the quality of welded joints and control of the FSW process: the speed of rotation of the tool, v_{rot}; welding speed, v_{wel}; vertical force to work materials, F; tool tilt-angle, α; tool-plunge depth, a; and tool geometry, /11-12/. Process parameters used for welding T-joints from the first phase of experimental work were in intervals: v_{wel} = 24–73 mm/min; v_{wel} = 600–950 rpm; a = 5.3–5.9 mm, and α = 0–1.5°. Process parameters used for welding T-joints from the second phase of experimental work were: v_{wel} = 27–60 mm/min; a = 5.6–5.8 mm; α = 1° and v_{rot} = 950 rpm.

Two methods were used for testing welded T joints: non-destructive and destructive. Non-destructive testing referred to the visual control of the face and root side of weld metal. Destructive testing included the macrostructure and micro-hardness tests. All tests are conducted in accordance with applicable standards.

RESULTS AND DISCUSSION

Visual control of the front and root sides of the weld metal was performed for all of the welded joints. During the experiment all welding stages are monitored. The welding process involved the occurrence of defects in weld metal as: tunnels, kissing bond, appearance of links during tool penetration, extrusion of softened material due to tool shoulder, sticking of the welded joints to the base plate, plate separating and more. Once the work plates have been properly clamped (Fig. 2), the stage of tool mandrel penetration into the work plates has followed (Fig. 3).

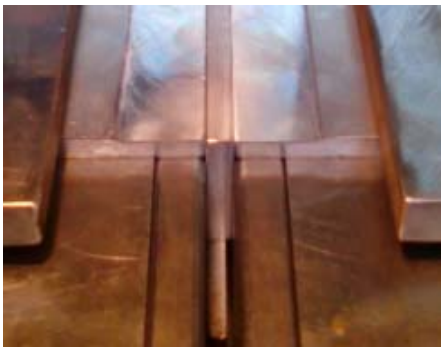

Figure 2. Plates clamped on the work table of the machine.

Figure 3. Penetration of the tool mandrel into the work plate.

The welding stage was monitored during the welding of each T-joint, Fig. 4. Figure 4a shows the smooth front surface with a slight flash of material retreating to the side of the weld metal. The flash is an occurrence that can be minimized by proper tool selection, although it cannot be eliminated, /8/. In addition, softened material extrusion due to the effects of the tool shoulder can be seen.

There was a problem with separating the plates during the welding of three plates, for both 5052-H32 and 5754-H111 alloys, as can be seen in Fig. 4b. Plates are separated due to great forces that occur during welding and insufficient clamping. It can be seen that a small link has spread over the welded joint front, due to tool penetration, as marked by the red ellipse.

The setbacks mentioned above occurred due to inadequate welding parameters, i.e. tool rotation speed, welding speed, tool tilt angle, pressure force, inadequate geometry of tool, depth of tool penetration and insufficient plate clamping.

The presence of an open tunnel on the advancing side (Fig. 5) is a result of an inadequate combination of welding parameters, /9/. The appearance (roughness) of the weld

front surface and the amount of extruded material around the tool shoulder is also heavily dependent on the applied welding parameters.

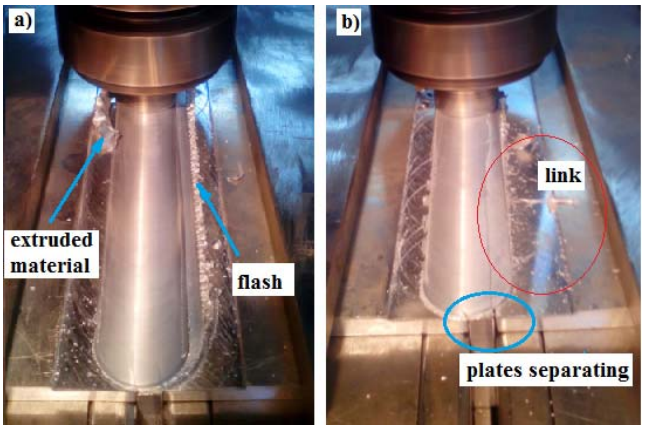

Figure 4. Problems during the FSW.

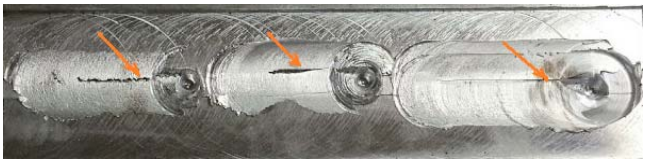

Figure 5. Open tunnels (red arrow) and a rough weld front surface.

Defects are not detected by visual control of the weld metal root side in T-joints. The appearance of the joint side is shown in Fig. 6. By observing the root side of the joint, it is possible to clearly identify the welding zone beneath the weld front.

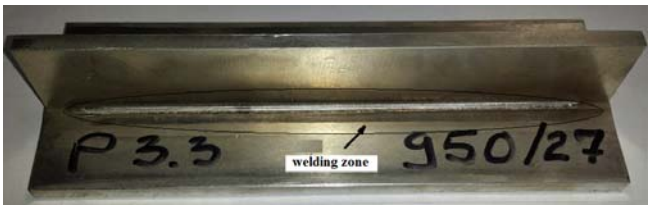

Figure 6. Root side of weld metal.

Distortion of one or both upper plates is observed on some T-joints in both welding phases. Distortion occurred due to the large welding forces, inadequate clamping of the working plates, and the high temperature of the process.

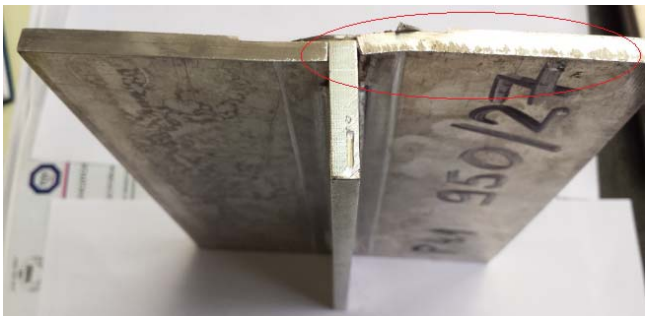

Figure 6. Examples of joint distortion.

Microhardness testing of T-joints is performed on joints with defects that were not detected by visual examination. Microhardness was tested through the welded joint cross-section perpendicular to the plate welding direction, in two directions: horizontal (near the face and root sides of the weld metal), and vertical (from the face to the root side of the weld metal, along the joint symmetry axis). In some T-joints the tunnel defect could be seen on the joint face, however, its presence could not have been confirmed with sufficient certainty. Measuring points for the microhardness test of a typical AA5052-H32 T-joint are shown in Fig. 7.

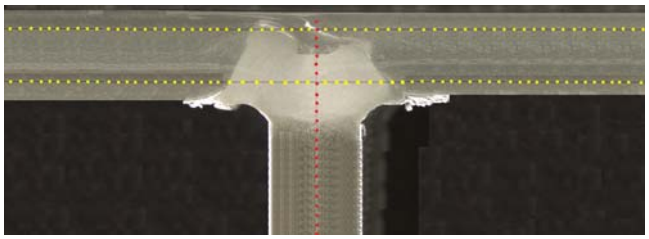

Figure 7. Measuring points for the microhardness test.

All diagrams for microhardness distribution of AA5052-H32 are similar and typical, as shown in Fig. 8.

Microhardness distribution through the cross-section measured in horizontal direction is not completely symmetrical relative to the joint central axis. Microhardness in the nugget area reached the value of hardness of the base material which was expected due to recrystallization and fragmentation of the structural grains. Sudden decrease in microhardness present in one of the imprints in the nugget area is observed. This is the consequence of a welded joint defect known as the bonding line, which can be seen more clearly in macroscopic images (Fig. 9).

Figure 8. Microhardness distribution for T-joint of AA5052-H32.

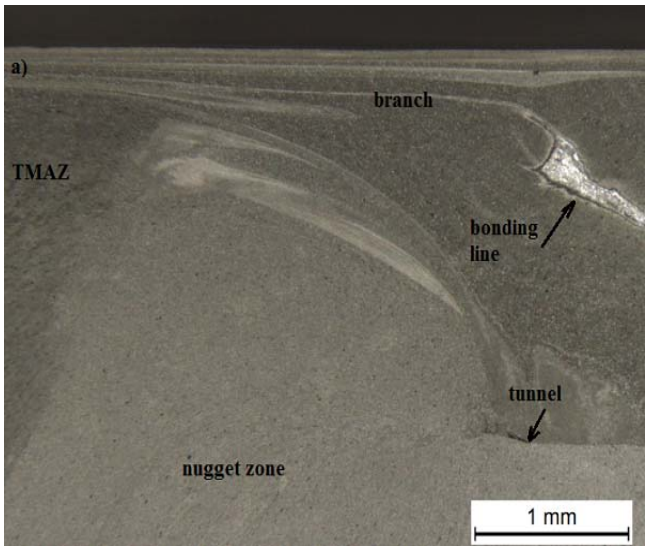

a) branch, nugget-TMAZ border on the advancing side, tunnel and bonding line

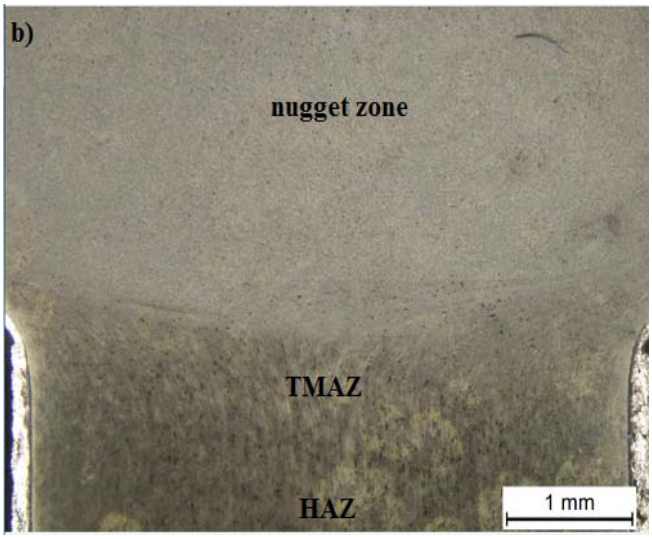

b) root side of weld metal, nugget-TMAZ-HAZ border

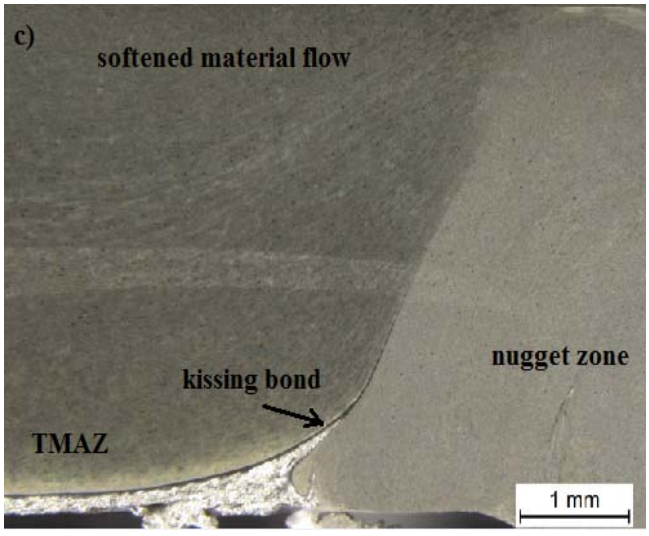

c) nugget-TMAZ border on the advancing side, kissing bond and observed lines of material flow

Figure 9. Macroscopic images of structural zones of the AA5052-H32 T-joint.

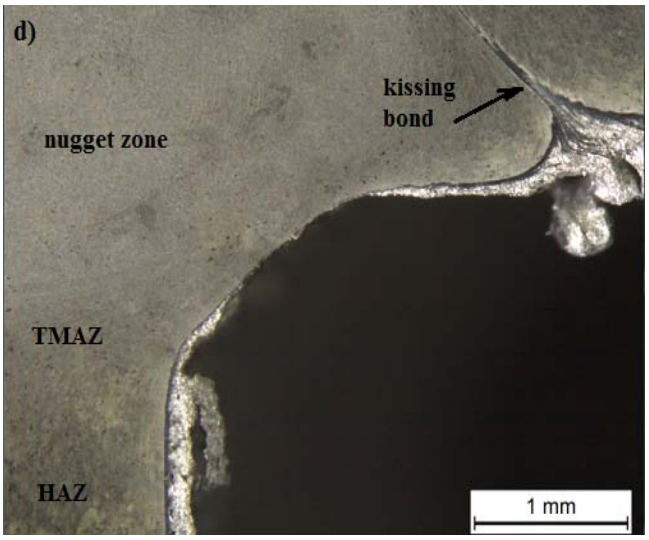

Figure 9. (continued) d) nugget-TMAZ-HAZ border on the retreating side, kissing bond.

There is some difference in the microhardness distribution diagrams in the vicinity of the front and root sides of the weld metal. In the nugget area and TMAZ, the hardness level near the weld front is significantly higher than the level at the root side of the weld, which is a result of insufficient material mixing due to the process temperature not being high enough. The material used for support plates in the first stage of experimental work is carbon steel, class S355, which lead to partial dissipation of heat from the welded zone which was necessary for the process to take place.

In the nugget area, the measured values of microhardness along the vertical direction correspond to the values measured along the horizontal direction near the root side of the weld, which is expected since the process temperature at this location is lowered due to heat dissipation through the base plates. The first two microhardness values, measured in a vertical direction (at 1 and 1.5 mm from the welded joint front), correspond to the values of microhardness measured along the horizontal direction near the welded joint front in the nugget area, since this is where the process temperature reached its highest constant value.

Welded T-joints of AA5052-H32 had approximately the same macroscopic images (Fig. 9), and all had the same types of defects.

A tunnel is observed on the advancing side of weld metal (Fig. 9a). This defect falls into the category of non-allowable defects since it results in a reduced cross-section. It occurs due to insufficient transport of softened material around the pin of the welding tool from the retreating-towards the advancing side, due to inadequate (too high) welding speed, /10-11/.

On the root side of the weld metal, in the immediate proximity of the nugget (Fig. 9c-d), type of defect kissing bond (imperfect bonding, incomplete penetration) can be observed. This defect occurs due to insufficient tool penetration and is significantly unfavourable since it represents an initial crack in the nugget which in turn reduces the tensile strength of the welded joint.

A bonding line is a type defect that is present on the advancing side. The ways in which these defects occur can be simply described in the following way: a thin oxide film located on the surfaces of two plates that are being welded which is not fully dispersed during the welding process. Shearing of the material due to the rotating tool mandrel, largely contributes to primary material flow, but very rarely in a vertical direction (secondary material flow). The presence of this defect on the advancing side indicates that the flow of material on that side is heavier, /12-14/. The bonding line represents an initial crack in the joint and thus its mechanical properties are reduced. This defect could have been avoided by employing a higher heat input into the process and by changing the tool geometry.

Another typical microhardness distribution along the horizontal and vertical directions throughout the cross-sections of the AA5754-H111 T-joint of is given in Fig. 10.

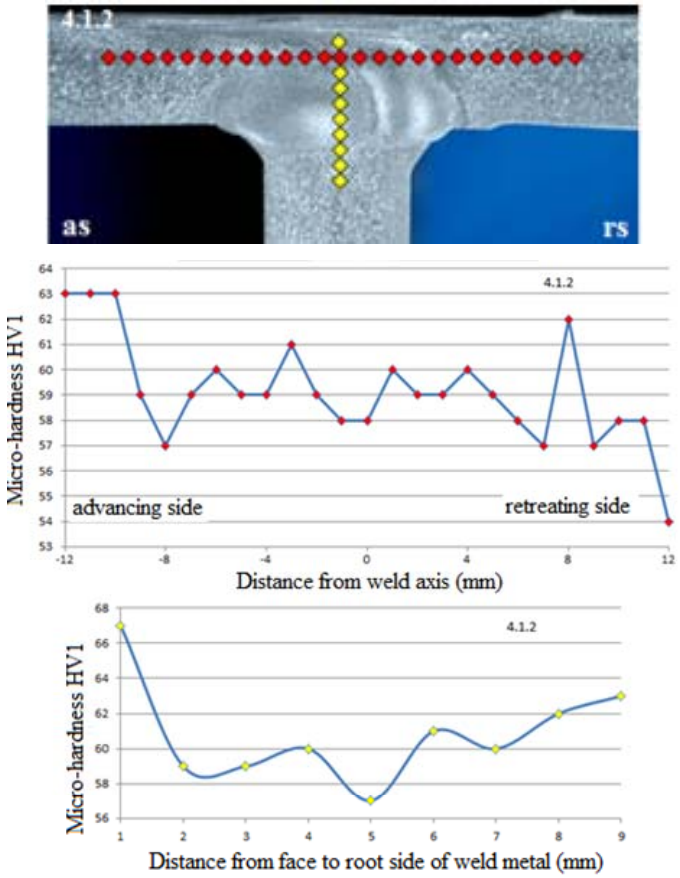

Figure 10. Microhardness distribution in AA5754-H111 T-joint.

Microhardness distribution diagrams along the horizontal direction through all welded T-joint cross-section are not symmetric relative to the joint centre. The highest measured values of microhardness are in the nugget area, whereas the lowest ones are in the TMAZ.

The largest decrease in hardness is recorded in the HAZ, closer to the thermo-mechanical zone. This change in hardness occurred due to the increase of structural grain during the increase of processing temperature.

In the nugget zone microhardness values measured in the vertical direction correspond to the values of microhardness measured in the horizontal direction. It is observed that the value of microhardness in the nugget zone are always larger near the face, than at the root of the weld metal. This is due to the higher temperatures of the process due from direct effects of the tool shoulder on the working plates.

T-joints of AA5754-H111 which are macroscopically examined do not have defects, as opposed to the joints made of AA5052-H32. The reason for this lies in the material clamping tool, since during the second phase of experimental work, stainless steel is used (and thus there is no temperature dissipation during the welding process). Characteristic macroscopic cross-section views of the welded T-joints (Fig. 11) are approximately the same.

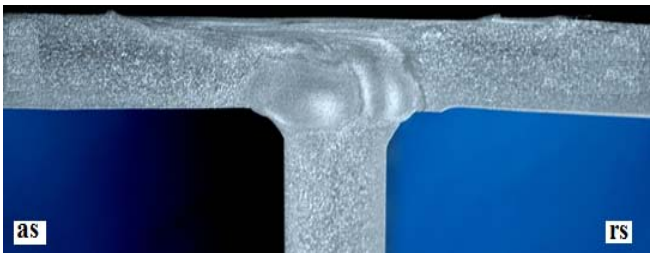

Figure 11. Macroscopic image of AA5754-H111 T-joint.

CONCLUSION

A tunnel defect type could not be seen by visual examination of welded AA5052-H32T-joints. Three types of defects are noticed by macroscopic examination of the structure in the T-joints cross-section: tunnel, incomplete penetration, and bonding line. These defects are caused by incorrect choice of welding parameters and they lack in the generated heat in the joining zone. The problem is that there is high heat conduction during the FSW process of T-joint. Heat conduction is largely determined by choice of material type of the backing plates and the clamping tool. In order to obtain defect-free T-joints with chosen welding parameters, the clamping tool material which is carbon steel should be replaced by a material that conducts less heat in the first phase of experimental welding.

Macroscopically examined AA5754-H111 T-joints are without imperfections. Stainless steel has proved to be a good material for backing plates and for the clamping tool when friction stir welding T-joints.

ACKNOWLEDGEMENT

This research is partially supported by the Ministry of Education, Science and Technological Development of the Republic of Serbia, through Grant project ON 174004.

REFERENCES

1. Mishra, R.S., Ma, Z.Y., *Friction stir welding and processing*, Mater. Sci. and Engng., 50(1-2): 1-78 (2005).
2. Mijajlović, M., Milćić, D., Đurđanović, M., Grabulov, B., Živković, A., Perović, M., *General terms in friction stir welding according to AWS D17.3/D17.3M:2010 and ISO 25239-1:2011 (in Serbian)*, Zavarivanje i zavarene konstrukcije (Welding and Welded Structures), 57(2): 61-6 (2012).
3. Grujić, M., Arakere, G., Pandurangan, B., Hariharan, A., Yen, C.-F., Cheeseman, B.A., *Development of a robust and cost-effective friction stir welding process for use in advanced military vehicles*, J of Mater. Engng. and Perf., 20(1): 11-13 (2011)

4. Živojinović, D., Fracture Mechanics Application to Structural Integrity Assessment of Aluminium Alloy Welded Structures, PhD Thesis in Serbian, University of Belgrade, Faculty of Mech. Engng., Belgrade, Serbia (2013).
5. Munoz, A.C., Ruckert, G., Huneau, B., Sauvage, X., Marya, S., *Comparison of TIG welded and friction stir welded Al-4.5 Mg-0.26Sc alloy,* J of Mater. Proc. Techn., 197: 337-343 (2008).
6. https://www.asm.matweb.com
7. https://www.alcoa.com/mill_products/europ
8. Đurđević, A., Sedmak, A., Živković, A., Đurđević, Đ., *Macro-structures, defects and microhardness of friction stir welded T-joints of AA 5052 and AA 5754-H111*, 7th Intl. Sci. and Expert Conf. TEAM 2015, 7(1): 523-527, Belgrade, Serbia (2015).
9. Dong, P., Lu, F., Hong, J.K., *Analysis of weld formation process in friction stir welding*, 1st Intl. Symp. on Friction Stir Welding, Thousand Oaks, Cal. (1999).
10. Peel, M.J., Steuwer, A., Withers, P.J., Dickerson, T., Shi, Q., Shercliff, H., *Dissimilar friction stir welds in AA5083-AA6082 Part I: Process parameter effects on thermal history and weld properties*, Metall. and Mater. Trans. A 37: 2183-2193 (2006).
11. Cao, X., Jahazi, M., *Effect of tool rotational speed and probe length on lap joint quality of friction stir welded magnesium alloy*, Mater. and Design, 32(1): 1-11 (2011).
12. Oosterkamp, A., Oosterkamp, L.D., Nordeide, A., *Kissing bond phenomena in solid-state welds of aluminium alloys*, Weld. J, 83(8): 225S-231S (2004).
13. Ren, S.R., Ma, Z.Y., Chen, L.Q., *Effect of initial butt surface on tensile properties and fracture behavior of friction stir welded Al-Zn-Mg-Cu alloy*, Mater. Sci. and Engng. A, 479: 293-299 (2008).
14. Schmidt, H.N.B., Dickerson, T.L., Hattel, J.H, *Material flow in butt friction stir welds in AA2024-T3*, Acta Mater., 54: 1199-1209 (2006).

ESIS ACTIVITIES

CALENDAR OF CONFERENCES & WORKSHOPS

June 19-24, 2016	21st Europ. Conf. on Fracture (ECF21)	Catania, Italy	http://www.ecf21.eu/
June 18-23, 2017	ICF14-Fourteenth International Conference on Fracture	Rhodes, Greece	http://www.icf14.org/
August 26-31, 2018	22nd European Conference of Fracture (ECF22)	Belgrade, Serbia	

Podsećamo Vas da su detaljnije informacije o radu Društva za integritet i vek konstrukcija dostupne na Internetu
http://divk.org.rs ili/or http://divk.inovacionicentar.rs

We remind You that more detailed information on the activities of the Society for Structural Integrity and Life are located on the Internet

INTEGRITET I VEK KONSTRUKCIJA
Zajedničko izdanje
Društva za integritet i vek konstrukcija (DIVK) i
Instituta za ispitivanje materijala

STRUCTURAL INTEGRITY AND LIFE
Joint edition of the
Society for Structural Integrity and Life and
the Institute for Materials Testing

http://divk.org.rs/ivk ili/or http://divk.inovacionicentar.rs/ivk/home.html

Cenovnik oglasnog prostora u časopisu IVK za jednu godinu
Pomažući članovi DIVK imaju popust od 40% navedenih cena.

Advertising fees for one subscription year–per volume
DIVK supporting members are entitled to a 40% discount.

Kvalitet*Quality	Dimenzije * Dimensions (mm)	Cene u din.	EUR
Kolor*Colour	• obe strane * two pages 2×A4	40.000	700
	• strana * page A4/1	25.000	450
	Dostava materijala: CD (Adobe Photoshop/CorelDRAW) Submit print material: CD (Adobe Photoshop/CorelDRAW)		
Crno/belo*Black/White	• strana * page A4/1	12.000	250
	• ½ str A4 * 1/2 page A4(18×12)	8.000	150
	Dostava materijala: CD (Adobe Photoshop/Corel DRAW) Submit print material: CD (Adobe Photoshop/Corel DRAW)		